An Open Publishing Platform of the Organization for Human Brain Mapping
APERTURE NEURO

ORIGINAL RESEARCH ARTICLE

Investigation of layer-specific BOLD signal in the human visual cortex during visual attention

Tim van Mourik[a*†], Peter J. Koopmans[b†], Lauren J. Bains[a], David G. Norris[a,b‡], Janneke F.M. Jehee[a*‡]

[a]Radboud University Nijmegen, Donders Institute for Brain, Cognition and Behaviour, Kapittelweg 29, 6525EN Nijmegen, The Netherlands
[b]Erwin L. Hahn Institute for Magnetic Resonance Imaging, Kokereiallee 7, D-45141 Essen, Germany

ABSTRACT

Directing spatial attention towards a particular stimulus location enhances cortical responses at corresponding regions in cortex. How attention modulates the laminar response profile within the attended region remains unclear, however. In this paper, we use high-field (7T) functional magnetic resonance imaging to investigate the effects of attention on laminar activity profiles in areas V1–V3 both when a stimulus was presented to the observer and in the absence of visual stimulation. Replicating previous findings, we find robust increases in the overall BOLD response for attended regions in cortex, both with and without visual stimulation. When analysing the BOLD response across the individual layers in visual cortex, we observed no evidence for laminar-specific differentiation with attention. We offer several potential explanations for these results, including theoretical, methodological and technical reasons. Additionally, we provide all data and pipelines openly in order to promote analytic consistency across layer-specific studies and improve reproducibility.

Keywords: layer specific, fMRI, cortical layers, visual attention, visual cortex, laminar activity

***For correspondence:** tim@timvanmourik.com (Tim van Mourik); j.jehee@donders.ru.nl (Janneke Jehee)

Contribution: †These authors contributed equally to this work.
‡These authors contributed equally to this work.

Date Received: June 6, 2021

Date Accepted: June 18, 2022

INTRODUCTION

Directing visual attention to a location in the visual field typically improves behavioural sensitivity to stimuli presented at that location (1–6). It is well known that these attentional benefits in behaviour are accompanied by increases in BOLD response in early visual areas (7–9), but the extent to which top-down processes and their cortical responses are reflected in BOLD at the laminar level remains less clear.

It is known from anatomical studies that the human cerebral cortex can be subdivided into histological layers with different cell types. The cytoarchitectonic structure varies across the brain and forms the basis of the Brodmann atlas (10). While the precise function of each cortical layer remains unclear, their connectivity profile suggests a division in terms of bottom-up and top-down processing (11–13). The grey matter in isocortex shows maximally six different histological layers. Specifically, Layer IV is associated with receiving feedforward signal from Layer III of lower cortical areas or from the thalamus (14, 15). Layers I–II and VI, in contrast, are typically implicated in receiving information flow from higher-level areas (feedback), which often originates from layers IIIa and VI (16). This bottom-up versus top-down connectivity profile of each of the layers is to some degree also paralleled in functional data. That is, from neurophysiological and neuroimaging work, it is known that various visual stimuli and tasks can exert differential effects on the various layers (17–21). Intracranial work in monkeys, for instance, shows that for selective attention and working memory (two functions that are commonly associated with top-down processes), current source density is increased in deep and superficial compared to middle layers in primary visual cortex (22). Similar layer-specific patterns have been shown in animal functional magnetic resonance imaging (fMRI). For instance, whisker stimulation led to an increase in BOLD response in Layer IV of rat barrel cortex, before such an enhancement was observed in any of the other layers, suggesting that Layer IV was the first to receive feedforward signal from upstream areas (23). In contrast, subsequent cortico-cortical

connections in the same task appeared to activate Layers II–III and V in the motor cortex and contralateral barrel cortex before this affected any of the other layers, suggesting that these layers were the first to receive feedback signals. To what extent these results generalise to human cortex, however, remains to be investigated.

Recent advancements in fMRI have made it possible to also investigate the functional role of cortical layers in humans (24–29). The human in vivo resolution with fMRI has increased to submillimetre voxel size. The thickness of the cerebral cortex varies between 1 and 4.5 millimetres (30, 31), giving sufficient resolution to characterise activity across the individual layers. fMRI is now often used to try and measure layer-specific activation in, for example, the visual system (27, 28, 32–34), the motor system (35), working memory tasks (36) and to find directional connectivity within and between language areas (29). If layer-specific analysis can make good on its promise of reliably discerning layer-specific signals, it can be useful for answering questions in a wide range of cognitive domains (37) and for questions of directional connectivity and cognitive network neuroscience (38), including research questions involving spatial attention.

Laminar fMRI data in humans can be acquired using gradient-echo (GE [24, 25]) or spin-echo (SE [39]) BOLD-based techniques or based on changes in CBV using the VASO method (35). GE-BOLD data are typically acquired with 2D or 3D-EPI (40), SE-BOLD with 2D spin-echo EPI or 3D GRASE (41), and VASO with a short TE GE-EPI readout, most commonly 3D-EPI (35, 40). The choice of technique involves a trade-off between sensitivity and efficiency against spatial specificity and has been discussed extensively (42, 43). GE-BOLD data can be acquired with high sensitivity and efficiency but suffers from vascular leakage caused by signal-recorded downstream from the point of activation. This problem can potentially be corrected post hoc by spatial deconvolution (44) or more sophisticated modelling (45) but is not present in spin-echo or VASO data. Our choice to use GE-BOLD contrast with a 3D-EPI readout was based on our earlier successful use of this technique in similar studies (27, 28) and is reinforced by more recent publications examining attentional modulation using this contrast (34, 46–49).

While some neurophysiological evidence suggests a differential involvement of the cortical layers in top-down attention (22, 50), the effects of attention on the different layers in human visual cortex has remained unclear. Here, we examine with fMRI the potential influence of spatial attention on BOLD activity in the deep, middle and superficial layers in human visual areas V1, V2, and V3. Participants directed their attention to a cued location and performed an attention-demanding task using an orientation stimulus that was shown at this location, while an unattended grating appeared at a different location of equal eccentricity. On some of the trials, subjects directed their attention to the cued location in anticipation of the stimulus, but no stimulus appeared at this location. We took care to optimise the experimental paradigm, the acquisition, the pre-processing pipeline, the number of subjects, and the statistical analysis to all be state of the art and tailored for an fMRI investigation at laminar resolution. Our expectation was to find deep-layer activation in a top-down (attention) condition and middle-layer activation in the bottom-up (stimulus) condition, in line with a substantial body of aforementioned histological, electrophysiological, and fMRI literature. Interestingly, although we observed a reliable increase of the overall BOLD response with attention across all layers, both with and without a stimulus present, we observed no differences in activation level between the layers due to attention. We provide several reasons for these findings in Discussion.To facilitate reproducibility of our results, we further include a reproducible and openly accessible processing pipeline for layer-specific analyses (https://doi.org/10.5281/zenodo.5559596 [51]). The toolbox includes benchmark tests for interactive visualisation of high-resolution coregistration, cortical lamination, and cardiac and respiratory noise filtering. To enhance transparency, the data analysis pipeline is furthermore presented as an online visual workflow that can be easily inspected, shared, and adapted to fit any laminar study's needs. As a result of the relative novelty of fMRI investigations into individual cortical layers, previous work has used a large variety of high-resolution toolboxes and analysis pathways (LAYNII in [35, 52]; OpenFmriAnalysis in [28]; Nighres in in [53]; BrainVoyager in [54]; AFNI in [55]), which has made direct comparison between studies difficult.

We hope that the availability of standard analysis pipelines such as this and others (34, 47) will help ameliorate this issue.

All code and fully anonymised data (time courses) are publicly available at https://doi.org/10.5281/zenodo. and require no authentication. Pre-processing of the data and construction of design matrices were performed in MATLAB. The finite impulse response (FIR) analysis, the region of interest analysis, and the layer-specific analyses were performed in a Jupyter notebook. The MRI image files are available in a Donders Data Repository and require authentication with an ORCID account (free) or a supported Dutch educational account. This is required by institutional regulations and European privacy legislation (GDPR). All data can be found online: https://doi.org/10.34973/bf42-rx14 for a full data set for a single subject and all raw files from the scanner (https://doi.org/10.34973/eb4d-md15). Layer-specific analysis was performed using custom-written software available online at https://github.com/TimVanMourik/OpenFmriAnalysis. This pipeline can be inspected graphically (51) (https://giraffe.tools/workflow/TimVanMourik/LayerAttention). Moreover, it can readily be applied to custom data; we prepared data from a representative subject to be used as a template pipeline.

RESULTS

We first describe the overall task effects that form the basis for our laminar-specific fMRI analysis. Our experimental paradigm is depicted in ***Figure 1*** and described in detail in Methods and Materials. In brief, we used an orientation discrimination task in order to investigate the (laminar-specific) effects of a visual stimulus and directed spatial attention. Analysis of the behavioural results showed that subjects generally performed well on the task. The mean orientation discrimination threshold across participants was 6.56° (standard error: 1.20°). The accuracy for directed attention to the left and to the right both stabilised quickly towards 80% in line with expectation. Figures of dynamic difficulty and accuracy over time are included in ***Figure 1–Figure Supplement 1 and Figure 1–Figure Supplement 2.***

Spatial attention increases fMRI response amplitudes

The experiment consisted of four experimental conditions: a two-by-two design in which we manipulated the effect of bottom-up visual stimulation, combined with an attentional manipulation across the two hemifields. The stimulus consisted of two orientation gratings presented to the left and right side of fixation. Participants were cued to attend to one location at either side of fixation. They performed a two-alternative-forced-choice task on the stimulus at the attended location, indicating whether its orientation was rotated clockwise or counterclockwise with respect to the nearest diagonal orientation. They maintained fixation on a central bull's-eye stimulus throughout the experiment. The design is described in detail in Methods and Materials and in ***Figure 1***. Prior to the experiment, participants trained the task in a separate behavioural session.

To benchmark the data, we first determined whether directing attention to a spatial location led to a stronger overall response in the visual cortex. Regions of interest consisted of voxels that were significantly activated by the stimulus in all layers of areas V1, V2, and V3 (see Methods and Materials). Visual areas were delineated using data acquired in a separate retinotopy session prior to the main experiment. We compared the amplitude of the BOLD response with and without attention, for trials in which a stimulus was presented and those in which no stimulus appeared on the screen (see ***Figure 2***). Data were analysed using a general linear model (GLM) with area, attention (attended vs. unattended), and stimulus (present vs. absent) as factors (see Methods and Materials).

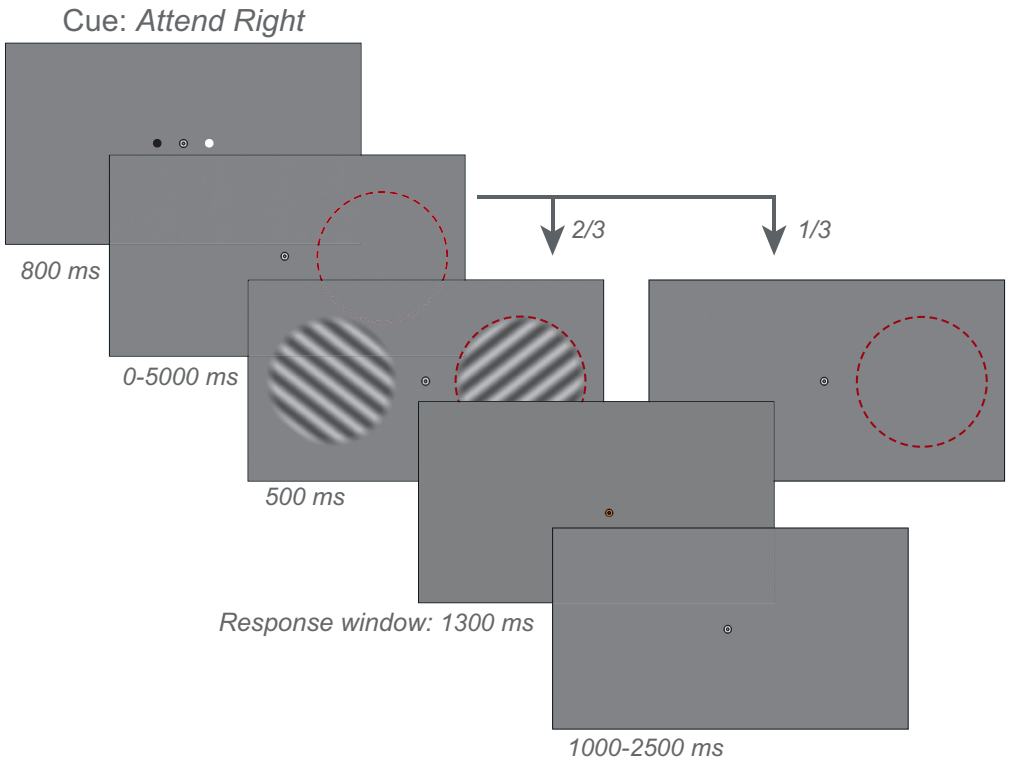

Fig 1. Stimuli and experimental procedure. Example of a trial sequence from the experiment. Subjects 1xated a central bull's eye target while gratings of independent orientation (± 45°) appeared in each hemi1eld. A compound black/white cue indicated whether subjects should attend to the left or right stimuli; in this example, the white circle indicates 'attend right'. Subjects had to discriminate near-threshold changes in orientation of the attended grating with respect to the closest diagonal. In one-third of trials, no stimuli appeared at either location. Red circles depict the attended location and were not present in the actual display.

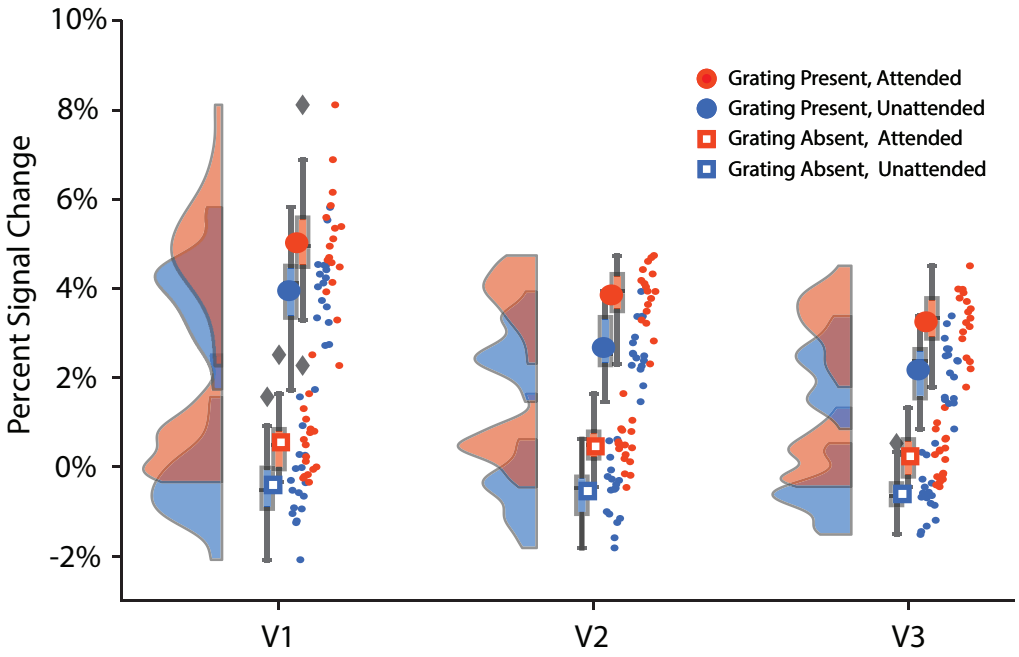

Fig 2. Amplitude of the BOLD response in areas V1–V3 for stimuli and locations that were either attended or ignored. Circles indicate when a grating was presented, and squares depict when no grating was presented at either the attended (red) or unattended (blue) location. When a stimulus was presented, activation reliably increased across all layers. Also attention significantly enhanced the BOLD response across all layers.

We first focused on the effects of attention per se. Attention significantly enhanced the BOLD response at the attended location in areas V1–V3 (effect of attention, $F(1, 16) = 121.3$, $p = 7.07 \bullet 10^{-9}$). The mean effect sizes (in per cent signal change) were 1.01%, 1.09% and 0.96% for V1, V2, and V3, respectively, and slightly stronger to those reported before (56–58). This increase in effect size is to be expected given that we imaged at 7T, whereas previous studies were done at 3T (59). To account for potential variation in baseline response between visual areas and to facilitate direct comparison with previous studies, we computed an attentional modulation index (AMI; [9]). The AMI is defined as the attentional effect divided by the response to the attended stimulus. We found AMIs ($\mu \pm \sigma$) of 0.18 ± 0.05 for V1, 0.24 ± 0.07 for V2, and 0.24 ± 0.09 for V3. Direct comparison between areas revealed that although the absolute contribution of attention did not change, the relative contribution of attention differed significantly between regions (AMI: $F(2, 32) = 10.53$, $p = 3.07 \cdot 10^{-4}$). Post hoc comparison showed significant differences in V1 compared to V2: $T(16) = -4.69$, $p = 2.44 \cdot 10^{-3}$ and in V1 compared to V3 $T(16) = -3.17$, $p = 5.89 \cdot 10^{-3}$, but not in V2 compared to V3: $T(16) = -0.14$, $p = 0.89$. Altogether, these results are in line with previously reported effects of attention on coarse-level BOLD activity in visual cortex (8, 60) and show that the cortical response for a spatial location is enhanced when attention is directed to that location.

Next, we investigated whether the effects of attention depended on the presence of a visual stimulus. Also in the absence of visual stimulation, there was a significant attention effect ($T(16) = 9.80$, $p = 3.64 \cdot 10^{-8}$), with mean effect sizes of 0.93%. We furthermore observed a slight negative BOLD response in the absence of visual stimulation and when the location was ignored ($T(16) = -3.12$, $p = 0.0066$). This result should be interpreted with caution, however, as the experiment did not include an attention-neutral condition, and responses were computed with respect to an implicit baseline response. We next compared attentional effects between trials in which observers were expecting a stimulus but none was presented and trials in which the stimulus did appear on the screen. We found that the effect of attention in areas V1–V3 was significantly different in the presence compared to the absence of visual stimulation (two-way interaction between attention and stimulus, $F(1, 16) = 6.63$, $p = 0.0204$). Specifically, in the presence of a stimulus, the attentional effect was slightly higher ($T(16) = 2.87$, $p = 0.0060$), with no reliable difference between areas (three-way interaction between stimulus, attention and area, $F(2, 32) = 0.324$, $p = 0.726$). Thus, attending to a spatial location clearly enhances the BOLD response at that location, even in the absence of visual stimulation, albeit that attentional effects were slightly reduced when no stimulus was presented to the observer.

To qualitatively assess the shape of the BOLD response over time and confirm the parameters of our GLM approach, we additionally conducted a FIR anal- ysis. The FIR analysis can be inspected and reproduced online in a Jupyter notebook (https://github.com/TimVanMourik/LayerAttention/blob/master/Notebooks/LayerFir.ipynb). We extracted BOLD response curves for each experimental condition (see ***Figure 3***) and observed clear and reliable effects of attention on the BOLD response that

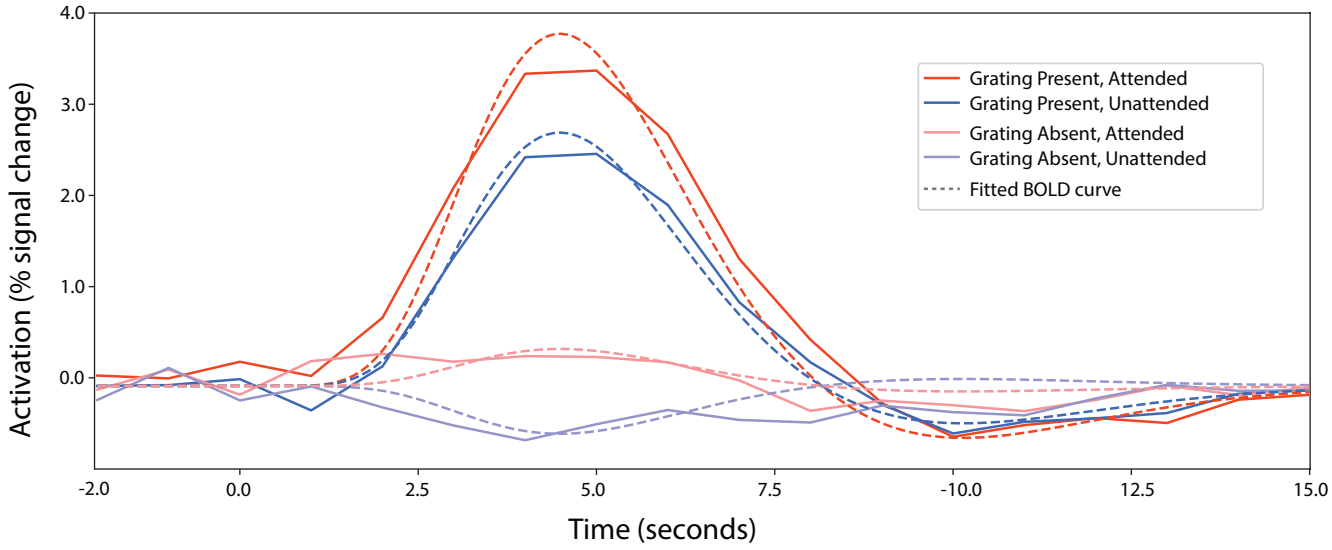

Fig 3. The fitted BOLD response for each experimental condition. The shaded area represents the standard error of the mean over subjects. Results were obtained by fitted a Finite Impulse Response function of 18 time points to the BOLD data, starting at 2 seconds before and running until 15 seconds after stimulus onset. The dashed line indicates an HRF that was fitted to the FIR results of a pilot session. The obtained parameter values were used in the modelled HRF across layers in our GLM analyses (see Methods). These results are averaged over hemisphere. Results for individual hemispheres are included in the supplemental materials.

were fully consistent with our previous analyses. Because of the left-right modulation of attention, attentional effects were reversed in the left and right hemisphere, as observed before and further illustrated in ***Figure 3–Figure Supplement 1***. Moreover, the cortical response over time for each condition was very well described by the canonical hemodynamic response function (HRF) ($r^2 = 0.982$ with attention and $r^2 = 0.985$ without attention). Thus, the HRF model presented an accurate description of the cortical responses observed in our experiment.

Spatial attention increases responses across the layers

Next, we asked whether attention led to changes in the pattern of activity across cortical layers. For each attention and stimulus condition, we first characterised the BOLD response over time for each of three distinct cortical layers in areas V1–V3 combined. Specifically, we used an FIR analysis to obtain the temporal laminar BOLD response profiles shown in ***Figure 4***. The analysis revealed clear hemodynamic response profiles that were well captured by the canonical HRF. In the presence of a stimulus, there appeared to be a progressive increase in response from the deep to the middle to the superficial layers, for both the stimulus and attention. In the absence of a stimulus, however, the layer-specific hemodynamic responses did not appear to show noticeable differences.

To assess the significance of these effects, data were analysed using a temporal general linear model with attention, stimulus, area, and layer as factors (see Methods and Materials). We found a reliable increase in BOLD response from white matter to pial surface (see ***Figure 5***, overall effect of cortical depth, $F(2, 32) = 87.5$, $p = 1.07 \cdot 10^{-13}$). This increase in BOLD response with decreasing distance to the pial surface was reliably larger in the presence of a stimulus (two-way interaction between layer and stimulus, $F(2, 32) = 85.6$, $p = 1.43 \cdot 10^{-13}$). Attention also led to reliable increases in BOLD response with decreasing distance to the pial surface (two-way interaction between layer and attention, $F(2, 32) = 43.10$, $p = 8.34 \cdot 10^{-10}$). This increase in BOLD response from lower to higher layers has been widely observed (24, 25, 35, 39, 61) and modelled previously and is consistent with increased baseline cerebral blood volume from the grey-white matter boundary towards the pial surface (45, 62). Due to this blood flow effect, a null ground truth (no laminar-specific effect) would yield increasing signal towards the surface due to carry-over signal towards downstream layers. The increase towards the surface is the statistical equivalent of an interaction effect of an experimental condition by layer, and it would be present even in the absence of a difference in neural activity.

Next, we determined whether the layer-specific increase in BOLD signal was different for attention-based effects compared to those of the visual stimulus. If so, then this would be consistent with a targeted effect of attention on one of the layers. Interestingly, the attention-based increase in activity was reliably different from stimulus-driven changes in layer response (post hoc comparison between layer by stimulus effect and layer by attention effect; $T(16) = 9.28$, $p = 7.64 \cdot 10^{-8}$). This could potentially reflect a specific effect of attention on one of the layers. However, there is also an alternative interpretation, as the magnitude of an interaction effect is tightly coupled to the strength of its main effects in layer-specific analyses. This is because the interaction effect can be interpreted as a difference in slope (signal by depths) between two lines. Due to cortical signal leakage as a result of physiological (blood flow) and methodological

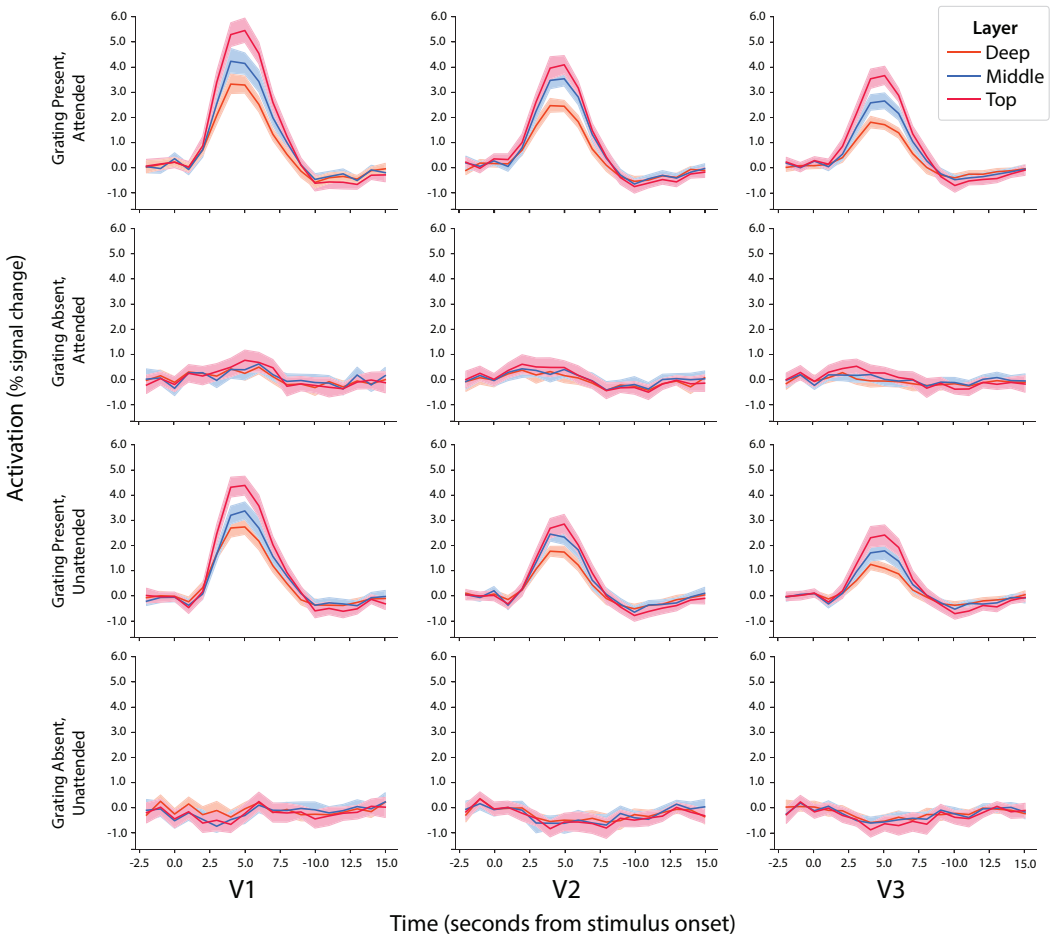

Fig 4. The fitted BOLD response for each experimental condition for three cortical layers. The shaded area represents the standard error of the mean over subjects. The horizontal axis represents time (in seconds) from stimulus onset.

reasons (errors in depth measurement), a higher visual stimulus response than an attentional response will be visible in both the main effect and the cortical slope of the response (see also above). Any reliable difference in slope is picked up as a significant difference between layer by stimulus effect and layer by attention effect. However, this difference in slope would also arise if there was no layer-specific change in neural activity, so this finding alone does not indicate conclusive layer-specific activation. Such conclusions might be made if a reliable three-way difference between the effects of attention and stimulus between any of the three layers would be present. Two identical slopes would yield a null effect for a three-way interaction, whereas a particular change in slope (e.g. an increasing slope for the stimulus-layer effect and a V-shaped pattern for the attention-layer effect) would yield a three-way interaction. However, we did not find a significant three-way interaction (three-way interaction between layer, stimulus and attention, $F(2, 32) = 0.96$, $p = 0.393$), making it difficult to draw any firm conclusions regarding the layer-specific effects of the stimulus versus attention.

While we observed no clear and unambiguous laminar differences across visual areas, it is possible that there could be a change within a given area. When analysing stimulus activity, the pattern of activity across the layers was, indeed, significantly different between the three areas (three-way interaction between layer, stimulus, area: $F(4, 64) = 3.10$, $p = 0.021$)). Post hoc analyses revealed that the stimulus response across layers was slightly steeper in V1 than V2 (stimulus by layer effect in area V1 compared to V2, $T(16) = 2.26$, $p = 0.038$), while no significant difference was observed for area V1 compared to area V3 ($T(16) = 1.35$, $p = 0.196$), or V2 compared to V3 ($T(16) = -1.43$, $p = 0.172$). This might reflect a slightly higher superficial layer activation in V1 compared to V2. On the other hand, it could also reflect the stronger main effect of stimulus in V1, leading to an increased slope of activation over layers, in line with expectations based on blood flow. We then focused on the layer-specific effects of attention in each individual area. However, we observed no layer-specific effects of attention per region (attention by layer by region effect $F(64, 4) = 0.998$, $p = 0.416$).

Thus, while the overall effects on BOLD activity of both visual stimuli and attention were robust and similar to previously reported values for visual cortex (9, 25, 57), both across and within layers, it proves more difficult to interpret the layer-specific pattern of activity for the two

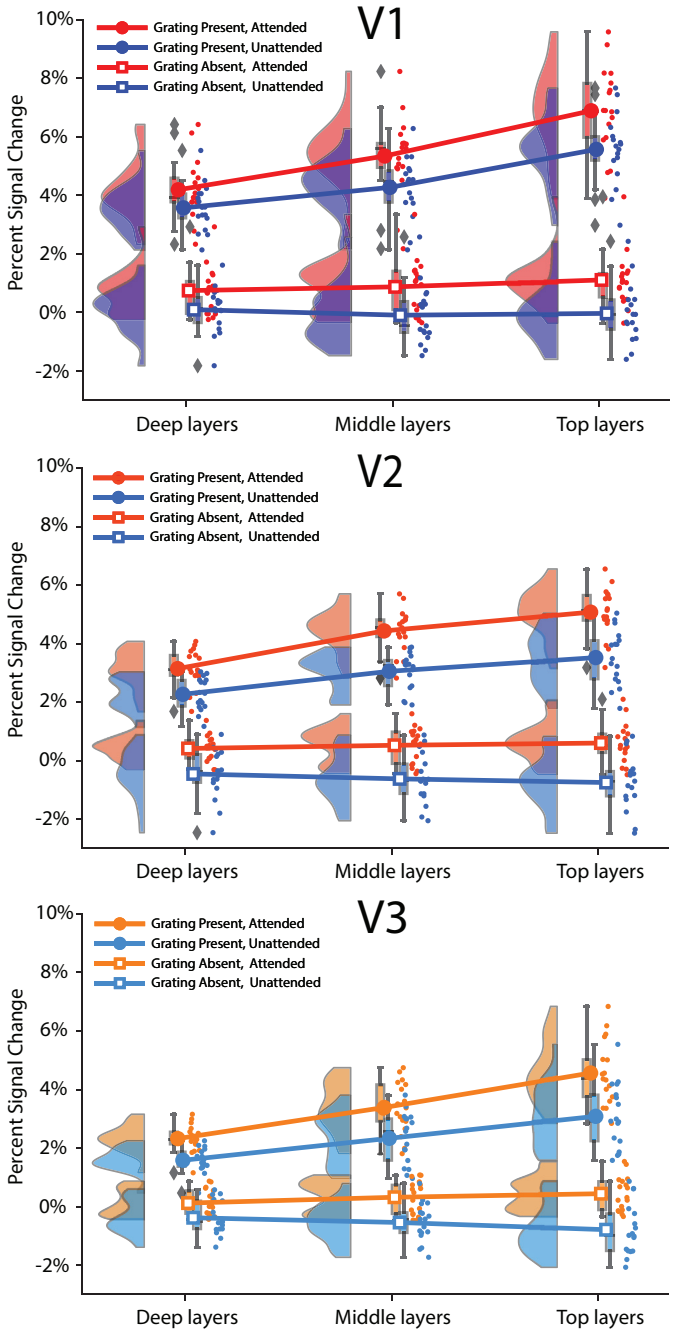

Fig 5. Layer-specific amplitude of the BOLD response in areas V1–V3 for stimuli and locations that were either attended or ignored. Circles indicate when a grating was presented, and squares depict when no grating was presented, at either the attended (red) or unattended (blue) location. When a stimulus was presented, activation reliably increased across all layers. Also attention significantly enhanced the BOLD response across all layers. Responses are shown as raincloud plots, which show an estimated distribution, boxplots (with grey diamonds as outliers), and individual responses.

conditions. Although at first sight, it may appear that the stimulus affected the layers in a manner different from attention (when analysed across areas), the effect should be interpreted with caution because the stimulus also led to a stronger coarse-level cortical response than attention. To rule out the possibility that some important parameter choices obscured true effects, we verified the robustness of our main results by changing the size of the region of interest and by varying the most important parameters of our layer extraction technique. We reprocessed the data and recomputed our layer- and region-specific statistical analysis for the experimental conditions. The control analyses established that the results were not strongly affected by the number of voxels included in the analyses ***(Figure 5–Figure Supplement 1 and Figure 5–Figure Supplement 2)*** nor by the number of layers analysed ***(Figure 5–Figure Supplement 3)***. In addition, the results did not qualitatively change when layer activation profiles were defined using volume interpolation (***Figure 5–Figure Supplement 4)***, as opposed to using a laminar spatial GLM as we did in the main analyses (see Methods and Materials). These control analyses and their comparison with the main analysis are further described in the supplemental materials. We also reanalysed the data in a Bayesian framework by means of a Bayesian repeated measures ANOVA (using JASP 0.14.10 [63]). As can be anticipated from the previous results, the best performing model is a model that includes the main stimulus, attention, cortical area, and layer effects, the interaction effects of layer with stimulus and attention, and a stimulus by cortical area interaction effect. Models with a layer by stimulus by attention effect had far lower probabilities. In line with previous work (28), we furthermore reanalysed the data after employing a z-scoring correction to the time courses. Although this led to small changes in area-specific effects of attention and stimulus, this did not lead to any significant layer-specific interaction in the ANOVA.

All figures and reported statistics for the main and control analysis are available as Jupyter Notebooks (https://doi.org/10.5281/zenodo.3428603). The (fully anonymised) BOLD time courses are included such that all results can be readily reproduced.

DISCUSSION

This study investigated the effects of spatial attention on the BOLD signal measured from individual layers in early visual cortex. Focusing first on the overall amplitude of the BOLD response in all layers combined, we found that attending to a stimulus reliably and substantially increased the BOLD signal in early visual areas, both when a stimulus was presented to the observer and in the absence of physical stimulation (9, 56, 64). Moreover, and much in line with earlier results on layer-specific activation patterns in visual cortex (24, 25), we observed a general increase in activation towards the superficial layers, which is likely caused by greater susceptibility to draining veins on the pial surface (61). Interestingly, and much to our surprise, we observed no forthright differential activity in the individual layers when comparing between top-down (attention-driven) and bottom-up (stimulus-driven) activities. We discuss several potential reasons for the discrepancy in findings mentioned below.

Why did we not find a targeted effect of attention on one of the layers? One possibility is that our data are simply insufficiently robust to show a significant difference in activity across depth between the two conditions. It is well known that the BOLD signal includes multiple sources of noise related to both MRI scanner and participant, and this holds especially true for signals recorded at the submillimeter scale. For example, at a high resolution, even the smallest movement of the participant may cause additional blurring of the data, with potentially detrimental effects on the signal-to-noise ratio. We collected data from 17 participants comparable to recent layer-based fMRI studies at high resolution (cf. $N = 12$ in (48), $N = 21$ in (28), $N = 22$ in [29], $N = 7$ and three sessions in [34], $N = 15$ [46]). To minimise the effects of various sources of noise, we took great care in measuring

and removing physiological artefacts and further improved the existing layer extraction techniques by developing a novel technique to separate laminar signal from different layers (65). Indeed, the combined success of these procedures is well illustrated by the effect sizes observed in the current study for both stimulus presentation (4.5%, 3.3%, and 2.8% in V1, V2 and V3) and attention (0.41%, 0.64%, and 0.59% in V1, V2 and V3), which are comparable or higher to those reported in previous work (56, 57). We also ensured that similar results were obtained using more conventional layer- extraction procedures and that the results were robust to changes in signal extraction method or number of layers. We did use an event-related design, which is known to be less sensitive than block designs (66). Shorter stimuli are also well known to exhibit a disproportionately large BOLD response (67, 68), and their laminar response can be expected to show an initial peak adjacent to the neuronal activity, followed by a lower downstream response towards the pial surface (45). Incorporating such a model in the analysis could potentially improve sensitivity but represents a development beyond the scope of this paper. In summary, although improvements in design and analysis could potentially have improved sensitivity, the effect sizes we observed lead us to the conclusion that the basic sensitivity of the experiment was not the reason for the absence of significant layer-specific attentional effects.

Because we were interested in the degree to which top-down processes could be dissociated from feedforward stimulation with fMRI, we directly contrasted between these two conditions in our analyses. Some previous studies, on the other hand, have focused on top-down activity in isolation (27, 28, 32). Others' experimental designs have independently manipulated attention and contrast similar to the two-by-two experimental designs employed by us (34, 37, 46). We emphasise that a multifactorial design is important to account for changes due to, for example, cortical depth and signal leakage per se, as opposed to true layer-based changes in activity due to the experimental manipulations. Alternate strategies are to compare between layers and conditions in terms of information content (32), retinotopic preference (48), or by focusing on inter-regional laminar communication (29). For example, Klein et al. (48) recently observed a cortical depth-dependent shift in population receptive fields with spatial attention. This raises the intriguing possibility that, in our study, spatial attention led to a depth-dependent shift in the strength of relatively fine-grained orientation-selective responses – indeed, previous coarse-scale fMRI studies have observed that orientation selectivity can change even when there is no change in amplitude across the population (57, 69).

A direct comparison with the studies most comparable to ours (34, 37, 46) is instructive to highlight both the similarities and differences. All studies have a GE-EPI acquisition, use similar spatial resolutions, and produce broadly similar laminar activation profiles. Lawrence et al. (37) showed an increased granular response with stimulus contrast and increased response for attention in superficial layers when comparing *z-scored time courses*. Liu et al. (46) modulated attention and used five different contrast conditions, and after a normalisation procedure found a strong attentional effect in superficial layers for V2–V3 and a weaker effect in both superficial and deep layers of V1. de Hollander et al. (34) found an effect of attention in superficial layers after spatial deconvolution. Neither the analysis of z-scored profiles nor spatial deconvolution (44) changed the outcome of our data, so it is unlikely that the differences are caused by the post-processing pipeline. All the studies did find an increased effect of attention in superficial layers, much like we do here, and indeed the study most similar to ours (34) similarly found no significant three-way interaction between layer, stimulus and attention. This leaves open the possibility that the conclusions drawn are perhaps more dissimilar than the results themselves.

We initially hypothesised that attention provides additional information about the stimulus (e.g. knowledge about its location). This information would come from higher-level areas and would presumably affect the deep or superficial layers. This was suggested by previous work using high-resolution fMRI focusing not only on spatial attention but rather figure-ground segmentation (27) and other extra-classical receptive field effects in cortex (32). However, our results are incongruent (insofar that they are comparable) and do not find similar effects for spatial attention. It is conceivable, however, that processes of perceptual grouping operate on the individual cortical layers in a manner different from the spatial attentional mechanisms studied here. It is known from primate studies, for example, that attention increases the response gain of neurons in visual cortex (70, 71) – such an increase in attentional gain could lead to general enhancements in neural activity irrespective of cortical layer, as we have observed here. This would offer a parsimonious explanation of both current and previous results.

To facilitate comparison between results, we have provided all our analysis code and data online (see Code and Data Availability).

METHODS AND MATERIALS

Participants

Nineteen healthy adults (aged 22–27, eight females), with normal or corrected-to-normal vision, participated in this study. All participants provided written informed consent in accordance with the guidelines of the local ethics committee (CMO region Arnhem-Nijmegen, the Netherlands, and ethics committee of the University Duisburg-Essen, Germany). Two subjects were excluded from analysis; one subject was excluded due to insufficient performance on the orientation discrimination task (their behavioural performance was at chance level) and another due to weak retinotopic maps. The remaining data from 17 subjects were analysed.

Experimental design and stimuli

Observers viewed the visual display through a mirror mounted on the head coil. Visual stimuli were generated by a Macbook Pro computer running MATLAB (2016B) and the Psychophysics Toolbox software (72, 73) and displayed on a rear-projection screen using a luminance-calibrated EIKI projector (resolution 1024 × 768 pixels, refresh rate 60 Hz). Participants were required to maintain fixation on a central bull's-eye target (radius: 0.25°) throughout each experimental run. Each run consisted of an initial fixation period (3000 ms) followed by 32 stimulus trials (average trial duration: 4.7 seconds). Trials were separated by inter-trial intervals of variable duration (1000–2500 ms, uniformly distributed across trials). Each trial started with the presentation of a central attention cue (800 ms). This was followed by a delay period of variable duration (0–5000 ms; drawn from an exponential distribution to ensure a constant hazard rate), after which the two orientation stimuli appeared on the screen (500 ms; two-thirds of trials). The orientation stimuli were followed by a response window (1300 ms), in which the fixation target turned orange, and observers indicated their response by pressing a button with their right index or middle finger. On one-third of the trials, no orientation stimuli appeared, and the screen remained blank for the remainder of the trial. A single trial of the experiment is illustrated in ***Figure 1***.

Stimuli were two counterphasing sinusoidal gratings of independent orientation ~45° or ~135°; size: 7°; spatial frequency: 1 cycle per degree; randomised spatial phase; contrast: 50%; contrast decreased linearly to 0 towards the edge of the stimulus over the last degree), centred at 5° to the left and right of fixation. We used a compound white/black cue consisting of two dots (dot size 0.25°) that straddled the fixation point (0.8° to the left and right of fixation) to indicate with 100% validity in which two gratings should be attended (57). Subjects were instructed to attend to the same side of fixation as either the white or black dot in the compound cue. Participants were instructed to detect a small clockwise or counterclockwise rotation in the orientation of the grating at the attended location with respect to a base orientation at 45° or 135°. The size of rotation offset was adjusted with an adaptive staircase procedure using QUEST (74), such that participants detected approximately 80% of the offsets correctly.

All but one participant completed 18 stimulus runs. The remaining participant completed 12 runs due to equipment failure. Retinotopic maps of visual cortex were acquired in a separate scan session at a 3T scanner using conventional retinotopic mapping procedures (75–77).

MR data acquisition

Functional images were acquired on a Magnetom Siemens 7T scanner with a 32-channel head coil (Nova Medical, Wilmington, USA) combined with dielectric pads ($CaTiO_3$; 175 × 110 × 10 mm^3, permittivity 110, conductivity 0.11 S/m) placed around the neck (78), using a T_{2*}-weighted 3D GE-EPI sequence (40). Matrix 232 × 232, FOV 192 × 192 mm, 72 slices oriented orthogonally to the calcarine sulcus, nominal voxel size 0.8 mm isotropic, GRAPPA factor 8 with 1/4 FOV caipi shift, 6/8 partial Fourier in both phase encoding dimensions, TE/TR = 20/51 ms, volume TR = 3060 ms, flip angle 14°, bandwidth 828 Hz/px, and echo spacing 1.37 ms. Gradient maximum amplitude was 40 mT/m (in practice, however, this maximum was not reached), and the maximum slew rate was 200 T/m/s. Shimming was performed using the standard Siemens shimming procedure for 7T. There were 18 runs of 72 ± 4 volumes, corresponding to an average of 3.7 minutes per run. The total average scan time per participant was 66 minutes. As the lengths of the events and the inter-trial interval were of unequal length, there was a small variation in the number of volumes per run.

Finger pulse was recorded using a pulse oximeter affixed to the index finger of the left hand. Respiration was measured using a respiration belt placed around the participant's abdomen.

Anatomical images were acquired using an MP2RAGE sequence (79). Matrix size 320 × 320, FOV 240 × 240 mm, slice thickness 0.75 mm, yielding two inversion contrasts (TR/TE/TI1/TI2 = 6000 ms/1.89 ms/800 ms/2700 ms), flip angles 4/5°.

In a separate session prior to the main experiment, a retinotopy session was conducted at a Siemens 3T Magnetom Trio scanner. A high-resolution T_1-weighted anatomical scan was acquired (MPRAGE, FOV 256 × 256, 1 mm isotropic voxels) at the start of the session. Functional images were subsequently collected using T_{2*}-weighted GE-EPI in 30 slices oriented perpendicular to the calcarine sulcus (TR/TE/α = 2000 ms/30 ms/90°, FOV = 64 × 64, [2.2 mm]^3 isotropic resolution).

Functional MRI pre-processing

Data pre-processing

Data were corrected for subject motion using SPM 12 with the mean functional volume across time as a reference (80). Residual motion-induced fluctuations in the BOLD signal were removed through linear regression based on the alignment parameters (three translation and three rotation parameters, no derivatives) of SPM. Scanner drifts were corrected via linear regression with high-pass filter regressors to filter out frequencies below 1/64 Hz. Pulsating signals as a result of the respiratory and cardiac cycle were removed as follows. The cardiac/respiratory peaks were automatically detected from the physiological recordings using in-house interactive peak-detection software and manually corrected where needed. With a custom MATLAB implementation of RETROICOR (81), fifth-order Fourier regressors were constructed for heart rate and respiration and subsequently removed from the functional images via linear regression. A small part (10% of respiratory measurements and 18% of heart rate measurements) was of insufficient quality and could not be used in this analysis. Functional data for these time frames were used in the main analysis but uncorrected for cardiac and respiratory noises.

The functional and anatomical scans were brought to the same space by registering the anatomical surface from the retinotopy session to the mean functional volume using boundary-based registration (BBR), implemented in FreeSurfer's bbregister (82) (FreeSurfer version 5.3). All registration results were inspected and manually refined when necessary. Where needed, registration was improved by an additional pass of BBR using an in-house MATLAB implementation (executed with MATLAB 2018b). Local distortions in EPI due to field inhomogeneity were corrected by means of recursive boundary registration (65), which recursively applies BBR to small portions of the cortical surface to correct topology locally by means of optimising the grey-white matter contrast along the surface. We used seven layers of recursion and only looked for translations and scalings in the phase encoding direction. Note that this procedure displaces the surface mesh and not the volume, so this has no smoothing effect on the (layer) signal.

Because of temporal changes in magnetic field inhomogeneity, local topology slightly changed over the course of the entire session. For this reason, the 18 functional runs obtained for each subject were first divided into three groups of each 6 contiguous runs, and then each group was pre-processed separately. Time courses were subsequently concatenated before entering the main analyses.

Regions of interest

Regions of interest (areas V1, V2, and V3) were defined on the reconstructed cortical surface using standard retinotopic mapping procedures (75–77). After identifying areas V1–V3, data from the main experiment were smoothed along the reconstructed cortical surface with a Gaussian kernel (FWHM: 4 mm). The smoothed version of the data was only used in region of interest selection and not in the main analysis. In each area, we then selected the 600 vertices that responded most strongly to the stimulus (shown on the cortical surface in ***Figure 5–Figure Supplement 5***). The selected vertices were resampled from the cortical surface back to subject space by means of FreeSurfer's label2vol. T-values of selected voxels ($\mu \pm \sigma$) were V1: $T = 2{,}989 \pm 0.854$, V2: $T = 2.317 \pm 0.689$, and V3: $T = 2.117 \pm 0.713$. Note that the selection of voxels based on visual activation per se is orthogonal to the analysis of interest, which addresses the effects of attention on individual layers in cortex. Control analyses verified that our results were not strongly affected by the number of vertices selected for subsequent analysis (***see Figure 5–Figure Supplement 1***).

Cortical profile extraction

Layer-specific signals were obtained by means of a layer-specific spatial GLM as described in detail and proposed by Van Mourik et al. (51). In brief, we obtained three equivolume layers, following the procedures described in (83). We took the reconstructed cortical surface as determined by FreeSurfer 5.3 (with the -hires option) (84) as a basis for this analysis. We used a custom implementation of (83) with mild adaptations: the gradient and the curvature of the cortex were defined as a function of Laplacian streamlines in the grey matter as this more naturally follows the structure of cortical columns (85). Partial volume inaccuracies were adjusted for by explicitly taking into account the orientation of the voxel with respect to the cortex (65).

The procedure enabled us to divide the grey matter in three equivolume cortical layers, which amount to roughly one voxel per layer. We additionally defined a volume on either side of these three cortical layers to capture signals for white matter and cerebrospinal fluid. On the basis of these definitions, we then computed a laminar mixing matrix of layer signal over the voxels (51). This was used as a spatial design matrix to unmix the layer signal. By means of a spatial regression of this matrix against the functional data within the ROIs, we obtained laminar time courses.

In separate control analyses, we verified that our laminar results did not qualitatively depend on the specific methods that were used to extract the laminar activation profile. We varied several parameters: the number of layers that we extracted and the method of obtaining laminar signal. For the former, we computed the cortical layers with the spatial GLM for four layers instead of three. For the latter, we computed the laminar signal based on a more conventional interpolation approach: by means of sampling the fMRI volumes at three cortical depths across the surface. This may contain contamination from other layers but is impervious to potential estimation errors as a result of the laminar spatial regression. The difference between approaches is described in detail in (51).

Temporal analysis

Temporal linear regression was used to compare between the experimental conditions. Regressors were created as follows. The stimuli appeared during the stimulus window on two-thirds of trials, which were modelled with a single regressor (stimulus on). The remaining stimulus windows were also modelled with a regressor (stimulus off). In addition, attention could be directed to either the left or right visual field; these conditions were each modelled with a regressor. We obtained four regressors for each of the conditions of interest. Thus, for a given retinotopic region of interest, the four different conditions were as follows: stimulus, no stimulus, attended, and unattended. We used a double-gamma function, as defined by SPM (parameters: time-to-peak first gamma: 5 seconds, time-to-peak second gamma: 10 seconds, amplitude ratio: 2:1) to model the fMRI responses. These parameters were established based on an initial FIR analysis (86) using the visual stimulus response from four pilot subjects (not included in the current study). Based on the observed fMRI response in this pilot data set, temporal or dispersion derivatives were not included into the statistical model of the main experiment. The baseline signal of each run was captured by adding a regressor column of ones for each run separately. As described above, the data were pre-processed by means of nuisance regression. This was performed by adding the nuisance regressors to the design matrix, effectively adjusting for the statistical loss in degrees of freedom as a result of nuisance regression.

We additionally performed an FIR analysis to qualitatively assess the BOLD response over time for each of the four conditions. This was used to confirm that the used HRF would accurately describe the true BOLD response. To visualise the cortical response over time for each of the four conditions, we analysed the data using FIR filters (86), applied to each layer. Specifically, we constructed FIR regressors for each of the four experimental conditions, each containing 18 time points that represented a time window of 1 second, starting 2 seconds before stimulus onset and running until 15 seconds thereafter.

We started at the level of the cortical region, initially with no further specification into layers. The temporal regressions were performed on the previously extracted time course of V1, V2, and V3. The obtained parameter estimates were divided by their baseline estimates in order to convert them to per cent signal change. These values were compared at the group level by means of ANOVAs and followed up with t-tests in case of significant effects. As the experiment was left-right symmetric and we found no differences between hemispheres in the analyses of interest, we used the 'attend left' and 'attend right' signal of the respective hemispheres as two measurements per participant.

We subsequently focused on the laminar level. For a qualitative assessment of the layer-specific BOLD response, we repeated the FIR analysis for each experimental condition and each layer. These qualitative results are shown in ***Figure 4***. The BOLD responses do not seem to vary per layer beyond a general intensity increase towards the pial surface. To further investigate this quantitatively, we repeated the region-specific analysis with the addition of the 'layer' factor. By means of an ANOVA, we ascertained layer-specific effects and their interactions with the stimulus and the region effects. These were followed by t-tests, where appropriate, to further inspect significant results. As the experiment was left-right symmetric and we found no differences between hemispheres in the analyses of interest, we took the hemisphere data as two measurements per participant.

As control analyses, we recomputed the layer-specific ANOVA in a Bayesian framework. The Bayesian analysis gives an indication of what model best explains the observed results with the least number of parameters, expressed as the likelihood of the models. We further recomputed the original ANOVA with two different pre-processing strategies. For the first, we applied a simple vascular model that should account for the blood flow effects towards downstream layers (44). The model describes that by approximation 20% of the layer signal seeps through to downstream layers. This can be accounted for by means of a spatial deconvolution. For the second, we z-scored the time courses per run (28), prior to the main analysis.

Code and data availability

All code and data can be found online: https://doi.org/10.34973/bf42-rx14 for a full data set for a single subject and https://doi.org/10.34973/eb4d-md15 for all raw files from the scanner. Layer- specific analyses were performed using custom-written software available online (https://github.com/TimVanMourik/OpenFmriAnalysis). This pipeline can be inspected graphically (51) (https://giraffe.tools/workflow/TimVanMourik/LayerAttention). Moreover, it can readily be applied to custom data; we prepared data from a representative subject to be used as a template pipeline.

Pre-processing of the data and construction of design matrices were performed in MATLAB. The FIR analysis, the region of interest analysis, and the layer-specific analyses were performed in an openly available Jupyter notebook (available at https://doi.org/10.5281/zenodo.3428603).

Author Contributions

PJK and JFMJ designed the experiment. TvM and LJB collected the data. TvM and DGN developed the laminar analysis techniques. TvM and JFMJ analysed the data. TvM, DGN, and JFMJ wrote the paper.

REFERENCES

1. Posner MI. Orienting of attention. Quarterly Journal of Experimental Psychology. 1980;32(1):3–25.
2. Lee DK, Koch C, Braun J. Spatial vision thresholds in the near absence of attention. Vision Research. 1997;37(17):2409–2418. Available from: http://www.sciencedirect.com/science/article/pii/S0042698997000552.
3. Yeshurun Y, Carrasco M. Attention improves or impairs visual performance by enhancing spatial resolution. Nature. 1998;396(6706):72–75. Available from: https://doi.org/10.1038/23936.
4. Carrasco M, Ling S, Read S. Attention alters appearance. Nature Neuroscience. 2004;7(3):308–313. Available from: https://doi.org/10.1038/nn1194.
5. Baldassi S, Verghese P. Attention to locations and features: Different top-down modulation of detector weights. Journal of Vision. 2005;5(6):556–570. Available from: https://doi.org/10.1167/5.6.7.
6. Ling S, Liu T, Carrasco M. How spatial and feature-based attention affect the gain and tuning of population responses. Vision Research. 2009;49(10):1194–1204. Available from: https://doi.org/10.1016/j.visres.2008.05.025.
7. Brefczynski JA, DeYoe EA. A physiological correlate of the 'spotlight' of visual attention. Nature Neuroscience. 1999;2(4):370–374. Available from: https://doi.org/10.1038/7280.
8. Gandhi SP, Heeger DJ, Boynton GM. Spatial attention affects brain activity in human primary visual cortex. Proceedings of the National Academy of Sciences of the United States of America. 1999;96(6):3314–3319. Available from: https://doi.org/10.1073/pnas.96.6.3314.
9. Kastner S, Pinsk MA, De Weerd P, Desimone R, Ungerleider LG. Increased activity in human visual cortex during directed attention in the absence of visual stimulation. Neuron. 1999;22(4):751–761. Available from: https://doi.org/10.1016/S0896-6273(00)80734-5.
10. Brodmann K. Vergleichende Lokalisationslehre der Großhirnrinde. Leipzig: Barth; 1909.
11. Felleman DJ, Van Essen DC. Distributed hierarchical processing in the primate cerebral cortex. Cerebral Cortex. 1991;1(1):1–47. Available from: https://doi.org/10.1093/cercor/1.1.1-a.
12. Barone P, Batardiere A, Knoblauch K, Kennedy H. Laminar distribution of neurons in extrastriate areas projecting to visual areas V1 and V4 correlates with the hierarchical rank and indicates the operation of a distance rule. The Journal of Neuroscience. 2000;20(9):3263. Available from: http://www.jneurosci.org/content/20/9/3263.abstract.
13. Shipp S. Neural elements for predictive coding. Frontiers in Psychology. 2016;7:1792. Available from: http://www.ncbi.nlm.nih.gov/pmc/articles/PMC5114244/.
14. Jones EG. Viewpoint: The core and matrix of thalamic organization. Neuroscience. 1998;85(2):331–345. Available from: http://www.sciencedirect.com/science/article/pii/S0306452297005812.
15. Constantinople CM, Bruno RM. Deep cortical layers are activated directly by thalamus. Science. 2013;340(6140):1591–1594. Available from: https://doi.org/10.1126/science.1236425.
16. Markov NT, Ercsey-Ravasz M, Van Essen DC, Knoblauch K, Toroczkai Z, Kennedy H. Cortical high-density counterstream architectures. Science. 2013;342(6158):1238406.
17. Maier A, Adams GK, Aura C, Leopold DA. Distinct superficial and deep laminar domains of activity in the visual cortex during rest and stimulation. Frontiers in Systems Neuroscience. 2010;4:31.
18. Xing D, Yeh CI, Burns S, Shapley RM. Laminar analysis of visually evoked activity in the primary visual cortex. Proceedings of the National Academy of Sciences of the United States of America. 2012;109(34):13871–13876.
19. Self MW, van Kerkoerle T, Super H, Roelfsema PR. Distinct roles of the cortical layers of area V1 in figure-ground segregation. Current Biology. 2013;23(21):2121–2129. Available from: http://www.sciencedirect.com/science/article/pii/S0960982213011299.
20. Vélez-Fort M, Rousseau CV, Niedworok CJ, Wickersham IR, Rancz EA, Brown APY, et al. The stimulus selectivity and connectivity of layer six principal cells reveals cortical microcircuits underlying visual processing. Neuron. 2014;83(6):1431–1443. Available from: http://www.sciencedirect.com/science/article/pii/S089662731400676X.
21. O'Herron P, Chhatbar PY, Levy M, Shen Z, Schramm AE, Lu Z, et al. Neural correlates of single-vessel haemodynamic responses in vivo. Nature. 2016;advance online publication. Available from: https://doi.org/10.1038/nature17965.
22. van Kerkoerle T, Self MW, Roelfsema PR. Layer-specificity in the effects of attention and working memory on activity in primary visual cortex. Nature Communications. 2017;8:13804.
23. Yu X, Qian C, Chen Dy, Dodd SJ, Koretsky AP. Deciphering laminar-specific neural inputs with line-scanning fMRI. Nature Methods. 2014;11(1):55–58.
24. Polimeni JR, Fischl B, Greve DN, Wald LL. Laminar analysis of 7T BOLD using an imposed spatial activation pattern in human V1. NeuroImage. 2010;52(4):1334–1346.
25. Koopmans PJ, Barth M, Norris DG. Layer-specific BOLD activation in human V1. Human Brain Mapping. 2010;31(9):1297–1304.
26. Maass A, Schütze H, Speck O, Yonelinas A, Tempelmann C, Heinze HJ, et al. Laminar activity in the hippocampus and entorhinal cortex related to novelty and episodic encoding. Nature Communications. 2014;5:5547. Available from: https://doi.org/10.1038/ncomms6547.
27. Kok P, Bains LJ, van Mourik T, Norris DG, de Lange FP. Selective activation of the deep layers of the human primary visual cortex by top-down feedback. Current Biology. 2016;26(3):371–376. Available from: https://doi.org/10.1016/j.cub.2015.12.038.
28. Lawrence SJ, van Mourik T, Kok P, Koopmans PJ, Norris DG, de Lange FP. Laminar organization of working memory signals in human visual cortex. Current Biology. 2018;28(21):3435–3440.
29. Sharoh D, Van Mourik T, Bains LJ, Segaert K, Weber K, Hagoort P, et al. Laminar specific fMRI reveals directed interactions in distributed networks during language processing. Proceedings of the National Academy of Sciences. 2019;116(42):21185–21190.
30. Zilles K. The human nervous system. San Diego: Academic Press; 1990.
31. Fischl B, Dale AM. Measuring the thickness of the human cerebral cortex from magnetic resonance images. Proceedings of the National Academy of Sciences of the United States of America. 2000;97(20):11050–11055. Available from: https://doi.org/10.1073/pnas.200033797.
32. Muckli L, De Martino F, Vizioli L, Petro LS, Smith FW, Ugurbil K, et al. Contextual feedback to superficial layers of V1. Current Biology. 2015;25(20):2690–2695. Available from: https://doi.org/10.1016/j.cub.2015.08.057.
33. Scheeringa R, Koopmans PJ, Van Mourik T, Jensen O, Norris DG. The relationship between oscillatory EEG activity and the laminar-specific BOLD signal. Proceedings of the National Academy of Sciences. 2016;113(24):6761–6766.
34. de Hollander G, van der Zwaag W, Qian C, Zhang P, Knapen T. Ultra-high field fMRI reveals origins of feedforward and feedback activity within laminae of human ocular dominance columns. NeuroImage. 2020;228:117683. Available from: http://www.sciencedirect.com/science/article/pii/S105381192031168X.
35. Huber L, Tse DHY, Wiggins CJ, Uludag K, Kashyap S, Jangraw DC, et al. Ultra-high resolution blood volume fMRI and BOLD fMRI in humans at 9.4T: Capabilities and challenges. NeuroImage. 2018;178:769–779. Available from: http://www.sciencedirect.com/science/article/pii/S1053811918305329.
36. Finn ES, Huber L, Jangraw DC, Molfese PJ, Bandettini PA. Layer-dependent activity in human prefrontal cortex during working memory. Nature Neuroscience. 2019;22(10):1687–1695.
37. Lawrence SJ, Formisano E, Muckli L, de Lange FP. Laminar fMRI: Applications for cognitive neuroscience. NeuroImage. 2019;197:785–791.
38. Huber L, Finn ES, Chai Y, Goebel R, Stirnberg R, Stöcker T, et al. Layer-dependent functional connectivity methods. Progress in Neurobiology. 2020;207:101835. Available from: http://www.sciencedirect.com/science/article/pii/S0301008220300903.
39. Olman CA, Harel N, Feinberg DA, He S, Zhang P, Uğurbil K, et al. Layer-specific fMRI reflects different neuronal computations at different depths in human V1. PLoS One. 2012;7(3):e32536.
40. Poser BA, Koopmans PJ, Witzel T, Wald LL, Barth M. Three dimensional echo-planar imaging at 7 Tesla. NeuroImage. 2010;51(1):261–266. Available from: https://doi.org/10.1016/j.neuroimage.2010.01.108.
41. Kemper VG, De Martino F, Vu AT, Poser BA, Feinberg DA, Goebel R, et al. Sub-millimeter T2 weighted fMRI at 7 T: Comparison of 3D-GRASE and 2D SE-EPI. Frontiers in Neuroscience. 2015;9:163.
42. Yang J, Huber L, Yu Y, Bandettini PA. Linking cortical circuit models to human cognition with laminar fMRI. Neuroscience & Biobehavioral Reviews. 2021;128:467–478.
43. Norris DG, Polimeni JR. Laminar (f)MRI: A short history and future prospects. NeuroImage. 2019;197:643–649. Available from: https://www.sciencedirect.com/science/article/pii/S1053811919303805.
44. Markuerkiaga I, Marques JP, Gallagher TE, Norris DG. Estimation of laminar BOLD activation profiles using deconvolution with a physiological point spread function. Journal of Neuroscience Methods. 2021;353:109095.
45. Havlicek M, Uludağ K. A dynamical model of the laminar BOLD response. NeuroImage. 2020;204:116209.
46. Liu C, Guo F, Qian C, Zhang Z, Sun K, Wang DJ, et al. Layer-dependent multiplicative effects of spatial attention on contrast responses in human early visual cortex. Progress in Neurobiology. 2020;207:101897.

47. Gau R, Bazin PL, Trampel R, Turner R, Noppeney U. Resolving multisensory and attentional influences across cortical depth in sensory cortices. Elife. 2020;9:e46856.
48. Klein BP, Fracasso A, van Dijk JA, Paffen CLE, te Pas SF, Dumoulin SO. Cortical depth dependent population receptive field attraction by spatial attention in human V1. NeuroImage. 2018;176:301–312. Available from: http://www.sciencedirect.com/science/article/pii/S1053811918303653.
49. Marquardt I, De Weerd P, Schneider M, Gulban OF, Ivanov D, Wang Y, et al. Feedback contribution to surface motion perception in the human early visual cortex. Elife. 2020;9:e50933.
50. Nandy AS, Nassi JJ, Reynolds JH. Laminar organization of attentional modulation in macaque visual area {V4}. Neuron. 2017;93(1):235–246. Available from: http://www.sciencedirect.com/science/article/pii/S0896627316308674.
51. Van Mourik T, Snoek L, Knapen T, Norris DG. Porcupine: A visual pipeline tool for neuroimaging analysis. PLoS Computational Biology. 2018;14(5):e1006064.
52. Huber L, Handwerker DA, Jangraw DC, Chen G, Hall A, Stüber C, et al. High-resolution CBV-fMRI allows mapping of laminar activity and connectivity of cortical input and output in human M1. Neuron. 2017;96(6):1253–1263.
53. Huntenburg JM, Steele CJ, Bazin PL. Nighres: Processing tools for high-resolution neuroimaging. GigaScience. 2018;7(7):giy082.
54. Goebel R. BrainVoyager—past, present, future. NeuroImage. 2012;62(2):748–756.
55. Schallmo MP, Weldon KB, Burton PC, Sponheim SR, Olman CA. Assessing methods for geometric distortion compensation in 7T gradient echo functional MRI data. Human Brain Mapping. 2021;42(13):4205–4223. Available from: https://onlinelibrary.wiley.com/doi/abs/10.1002/hbm.25540.
56. Murray SO. The effects of spatial attention in early human visual cortex are stimulus independent. Journal of Visualization. 2008;8(10):1–11. Available from: https://doi.org/10.1167/8.10.2.
57. Jehee JF, Brady DK, Tong F. Attention improves encoding of task-relevant features in the human visual cortex. Journal of Neuroscience. 2011;31(22):8210–8219. Available from: https://doi.org/10.1523/JNEUROSCI.6153-09.2011.
58. Sprague TC, Serences JT. Attention modulates spatial priority maps in the human occipital, parietal and frontal cortices. Nature Neuroscience. 2013;16(12):1879.
59. van der Zwaag W, Francis S, Head K, Peters A, Gowland P, Morris P, et al. fMRI at 1.5, 3 and 7 T: Characterising BOLD signal changes. NeuroImage. 2009;47(4):1425–1434.
60. Somers DC, Dale AM, Seiffert AE, Tootell RB. Functional MRI reveals spatially specific attentional modulation in human primary visual cortex. Proceedings of the National Academy of Sciences of the United States of America. 1999;96(4):1663–1668.
61. Koopmans PJ, Barth M, Orzada S, Norris DG. Multi-echo fMRI of the cortical laminae in humans at 7 T. NeuroImage. 2011;56(3):1276–1285.
62. Markuerkiaga I, Barth M, Norris DG. A cortical vascular model for examining the specificity of the laminar {BOLD} signal. NeuroImage. 2016;132:491–498. Available from: http://www.sciencedirect.com/science/article/pii/S1053811916001919.
63. Marsman M, Wagenmakers EJ. Bayesian benefits with JASP. European Journal of Developmental Psychology. 2017;14(5):545–555.
64. Li X, Lu ZL, Tjan BS, Dosher BA, Chu W. Blood oxygenation level-dependent contrast response functions identify mechanisms of covert attention in early visual areas. Proceedings of the National Academy of Sciences of the United States of America. 2008;105(16):6202–6207.
65. Van Mourik T, Van der Eerden JP, Bazin PL, Norris DG. Laminar signal extraction over extended cortical areas by means of a spatial GLM. PLoS One. 2019;14(3):e0212493.
66. Friston KJ, Zarahn E, Josephs O, Henson RN, Dale AM. Stochastic designs in event-related fMRI. NeuroImage. 1999;10:607–619.
67. Yeşilyurt B, Uğurbil K, Uludağ K. Dynamics and nonlinearities of the BOLD response at very short stimulus durations. Magnetic Resonance Imaging. 2008;26:853–862.
68. Vazquez AL, Noll DC. Nonlinear aspects of the BOLD response in functional MRI. NeuroImage. 1998;7:108–118.
69. Jehee JF, Ling S, Swisher JD, van Bergen RS, Tong F. Perceptual learning selectively refines orientation representations in early visual cortex. Journal of Neuroscience. 2012;32(47):16747–16753.
70. Treue S, Trujillo JCM. Feature-based attention influences motion processing gain in macaque visual cortex. Nature. 1999;399(6736):575–579. Available from: https://doi.org/10.1038/21176.
71. Martinez-Trujillo JC, Treue S. Feature-based attention increases the selectivity of population responses in primate visual cortex. Current Biology. 2004;14(9):744–751. Available from: http://www.sciencedirect.com/science/article/pii/S0960982204002684.
72. Brainard DH. The psychophysics toolbox. Spatial Vision. 1997;10:433–436.
73. Pelli DG. The VideoToolbox software for visual psychophysics: Transforming numbers into movies. Spatial Vision. 1997;10:437–442.
74. Watson AB, Pelli DG. Quest: A Bayesian adaptive psychometric method. Perception & Psychophysics. 1983;33:113–120.
75. Sereno MI, Dale A, Reppas J, Kwong K, Belliveau JW, Brady TJ, et al. Borders of multiple visual areas in humans revealed by functional magnetic resonance imaging. Science. 1995;268(5212):889–893.
76. DeYoe EA, Carman GJ, Bandettini P, Glickman S, Wieser J, Cox R, et al. Mapping striate and extrastriate visual areas in human cerebral cortex. Proceedings of the National Academy of Sciences. 1996;93(6):2382–2386.
77. Engel SA, Glover GH, Wandell BA. Retinotopic organization in human visual cortex and the spatial precision of functional MRI. Cerebral Cortex. 1997;7(2):181–192.
78. Teeuwisse WM, Brink WM, Webb AG. Quantitative assessment of the effects of high-permittivity pads in 7 Tesla MRI of the brain. Magnetic Resonance in Medicine. 2012;67(5):1285–1293.
79. Marques JP, Kober T, Krueger G, van der Zwaag W, Van de Moortele PF, Gruetter R. MP2RAGE, a self bias-field corrected sequence for improved segmentation and T1-mapping at high field. NeuroImage. 2010;49(2):1271–1281. Available from: http://dx.doi.org/10.1016/j.neuroimage.2009.10.002.
80. Friston K, Ashburner J, Frith CD, Poline JB, Heather JD, Frackowiak RS, et al. Spatial registration and normalization of images. Human Brain Mapping. 1995;3(3):165–189.
81. Glover GH, Li TQ, Ress D. Image-based method for retrospective correction of physiological motion effects in fMRI: RETROICOR. Magnetic Resonance in Medicine. 2000;44(1):162–167.
82. Greve DN, Fischl B. Accurate and robust brain image alignment using boundary-based registration. NeuroImage. 2009;48(1):63–72. Available from: http://www.sciencedirect.com/science/article/pii/S1053811909006752.
83. Waehnert MD, Dinse J, Weiss M, Streicher MN, Waehnert P, Geyer S, et al. Anatomically motivated modeling of cortical laminae. NeuroImage. 2014;93 Pt 2:210–220.
84. Dale AM, Fischl B, Sereno MI. Cortical surface-based analysis: I. Segmentation and surface reconstruction. NeuroImage. 1999;9(2):179–194. Available from: http://www.sciencedirect.com/science/article/pii/S1053811998903950.
85. Leprince Y, Poupon F, Delzescaux T, Hasboun D, Poupon C, Rivière D. Combined Laplacian-equivolumic model for studying cortical lamination with ultra high field MRI (7T). In: 2015 IEEE 12th International Symposium on Biomedical Imaging (ISBI); 2015:580–583.
86. Friston KJ, Fletcher P, Josephs O, Holmes A, Rugg M, Turner R. Event-related fMRI: Characterizing differential responses. NeuroImage. 1998;7(1):30–40.

APPENDIX

LAYER-SPECIFIC HRF FOR ALL CONDITIONS AND LAYERS

To assess the degree to which the results are robust to different analysis choices, we additionally analysed the data using a variety of alternative methodological parameters. This section discusses the obtained results. Our main analysis was done on a region of interest of 600 vertices. The method of extracting cortical signal was the spatial GLM (65) with three cortical layers. We redid the main analysis with a smaller region of interest (300 vertices) and a larger one (900 vertices), other factors remaining equal. We further wanted to make sure that changing the number of layers did not qualitatively change our interpretation and recomputed the main analysis with four instead of three cortical layers. For comparison with traditional studies that use signal interpolation for obtaining laminar signal, we also employed this technique in an additional control analysis. All results (p-values) of the main analysis, the ANOVA of the factors stimulus, attention, layer, and region, are included in one table (1).

For further inspection, the results are also included as figures, analogous to ***Figure 5*** in the main text. ***Figure 5–Figure Supplement 1 and Figure 5–Figure Supplement 2*** show stimulus and attention- based effects across layers after selecting, respectively, the 300 and 900 most activated vertices (cf. ***Figure 5*** in the main text, based on 600 vertices). Note that, per this selection, these results should (and do) show higher and lower activation values for the top 300 and 900 vertices, respectively. ***Figure 5–Figure Supplement 3*** shows results after defining four cortical layers, rather than three, and ***Figure 5–Figure Supplement 4*** depicts results obtained from interpolation instead of a laminar spatial GLM. Error bars indicate ±1 SEM. In all figures, presenting a stimulus (circles) resulted in a reliable increase in BOLD response from deep to superficial layers. The BOLD response was significantly enhanced for the attended (red) compared to unattended location (blue) across layers, both when a stimulus was presented and in the absence of visual stimulation (see Appendix Table 1 for statistics).

We repeated the main analysis four additional times. Thus, it is to be expected that some p-values that are around the significance threshold in the main analysis fall slightly below or rise slightly above it in some of the control analyses. There were only two instances where significance ($p < 0.05$) changed compared to the layer analyses that are presented in the main text.

While we observed a trending effect for the stimulus by attention interaction in the main laminar analysis (trending, with $p = 0.0733$), it was significant for the analysis with a larger ROI ($p = 0.0272$) and with four extracted layers ($p = 0.0118$), but not for the smaller ROI ($p = 0.271$) and trending for the signal extraction by means of interpolation ($p = 0.0552$). These results are all close together and hovering around the significance threshold of $p = 0.05$. A stimulus by attention effect ought to be interpreted as a multiplicative effect of stimulus and attention, that is, an additional signal increase when the presented stimulus is attended compared to when the location per se (i.e. no stimulus) is attended. However, this trending effect does not affect any of our conclusions regarding the layer-specific effects of stimulus and attention.

While the stimulus by layer by area interaction was significant in the main analysis ($p = 0.0214$), this interaction was not significant after selecting the 300 most activated vertices ($p = 0.2056$). However, in the three other control analyses, the effect became more pronounced (larger ROI: $p = 8.89 \cdot 10^{-3}$, interpolation: $p = 2.78 \cdot 10^{-5}$, and four layers: $p = 6.19 \cdot 10^{-4}$).

Appendix Table 1. The p-values for the ANOVA as described in the body of the paper. The five columns are the main analysis (first column, bold face) and four control analyses: an analysis based on a smaller ROI (300 vertices); on a larger ROI (900 vertices); the same ROI but laminar signal extracted by means of interpolation instead of a GLM; and a GLM but with four layers instead of three.

	GLM, 600 vertices	GLM, 300 vertices	GLM, 900 vertices	Interpolation	GLM, 4 Layers
Stimulus	**1.648436e-12**	5.954187e-13	1.290311e-11	3.726032e-12	2.496749e-13
Attention	**1.032463e-08**	3.833341e-08	4.175371e-09	9.482100e-09	9.216548e-09
Layer	**1.067460e-13**	2.851381e-11	7.013292e-13	1.890989e-15	3.237563e-15
Area	**1.134083e-08**	2.712885e-08	1.114299e-07	1.019932e-08	4.101310e-09
Hemisphere	**9.914955e-01**	9.461482e-01	9.101537e-01	9.177039e-01	9.029095e-01
Stimulus:Attention	**7.331790e-02**	2.710442e-01	2.720432e-02	5.523979e-02	1.179676e-02
Stimulus:Layer	**1.433143e-13**	6.233730e-12	7.235421e-14	8.002511e-15	2.812629e-18
Attention:Layer	**8.335165e-10**	3.172532e-08	1.934224e-10	7.100456e-12	2.061512e-11
Stimulus:Area	**9.424679e-10**	2.786488e-08	7.976153e-09	7.472970e-10	1.449285e-10
Attention:Area	**7.253885e-02**	1.208362e-01	7.744268e-02	1.406810e-01	8.801709e-02
Layer:Area	**8.137692e-04**	3.749919e-03	7.251511e-03	1.577094e-05	9.033174e-02
Stimulus:Attention:Layer	**3.936910e-01**	7.659098e-01	1.507279e-01	7.908435e-02	5.661013e-01
Stimulus:Attention:Area	**7.370581e-01**	6.246065e-01	7.617405e-01	7.980477e-01	7.956297e-01
Stimulus:Layer:Area	**2.136465e-02**	2.055745e-01	8.894002e-03	2.779890e-05	6.190268e-04
Attention:Layer:Area	**4.155126e-01**	2.893327e-01	3.384936e-01	2.462276e-01	3.289884e-01
Stimulus:Attention:Layer:Area	**8.124587e-01**	8.742156e-01	7.084470e-01	9.209281e-01	1.570871e-01

Note: *p*-Values above 0.05 are marked in black. *p*-Values between 0.05 and 0.01 are marked in red. *p*-Values below 0.01 are marked in green.

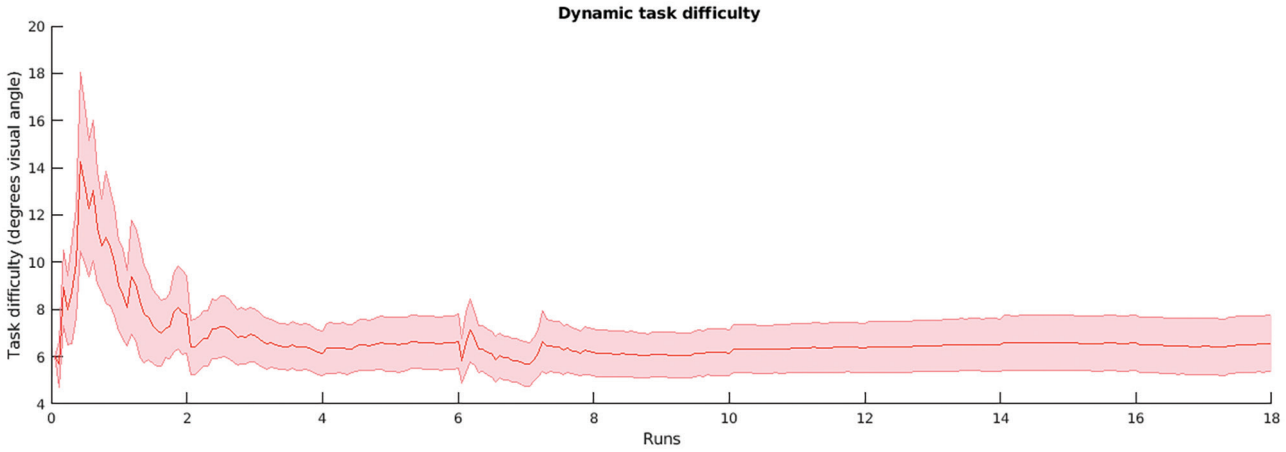

Figure 1–Figure supplement 1. Dynamically adjusted task diZculty, based on the subject's performance. Task diZculty is measured in degree visual angle and was dynamically adjusted such that participants scored at 80% accuracy. The 1gure shows the mean diZculty with the standard error of the mean as shaded area. The Bayesian strategy to update the parameters has high variance in the beginning as a result of limited available information. After six and twelve runs, there was a short break of the task to acquire a 1eld map, after which the task resumed. This probably relates to the mild drop in accuracy at the start of run six.

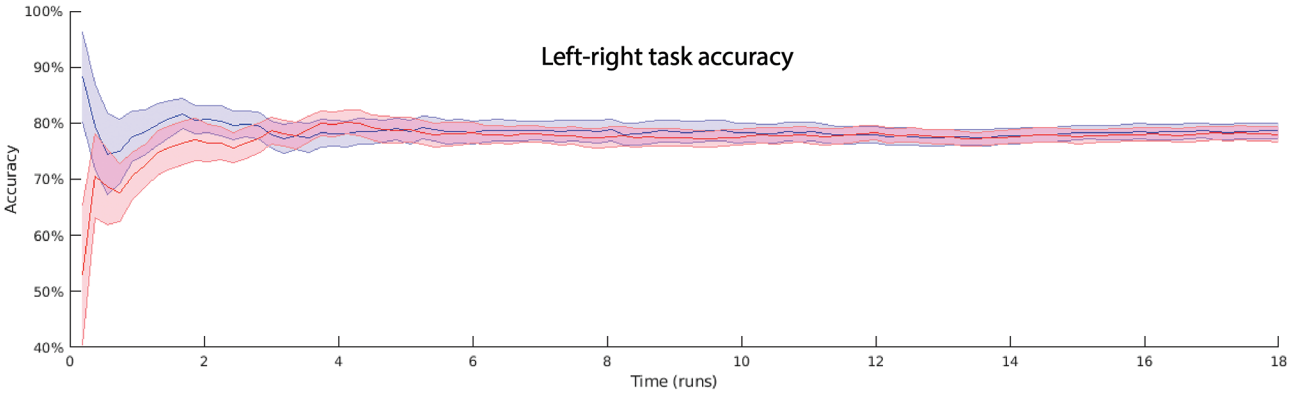

Figure 1–Figure supplement 2. Behavioural performance over the course of the experiment, expressed in percentage correct. This was calculated separately for trials in which attention was directed to the right, and trials in which attention was directed to the left. The initial high variance is to be expected as there are few trials and scores towards 0% and 100% are likely. Both accuracies then stabilise towards 80%, which was indeed the target accuracy of the experiment.

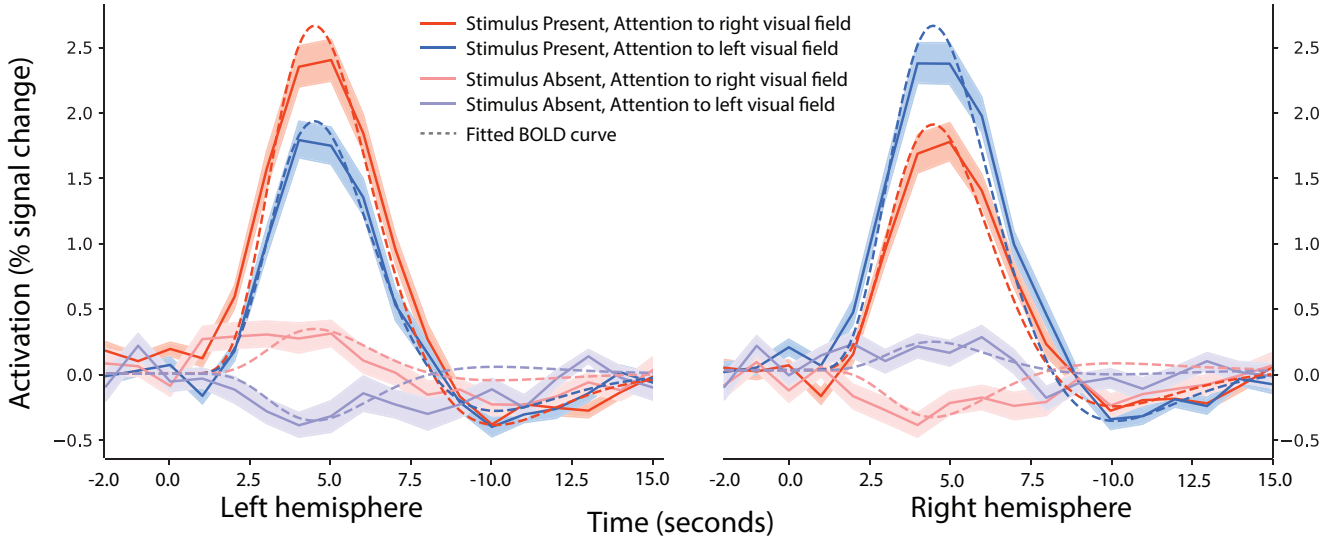

Figure 3–Figure supplement 1. The fitted BOLD response for each experimental condition, separated by hemisphere. The shaded area represents the standard error of the mean over subjects. Results were obtained by fitting a finite impulse response function of 18 time points, starting at 2 seconds before and running until 15 seconds after stimulus onset. The dashed line indicates an HRF that was fitted to the responses in a pilot session (see Methods and Materials). The same HRF parameter values were used in other statistical analyses.

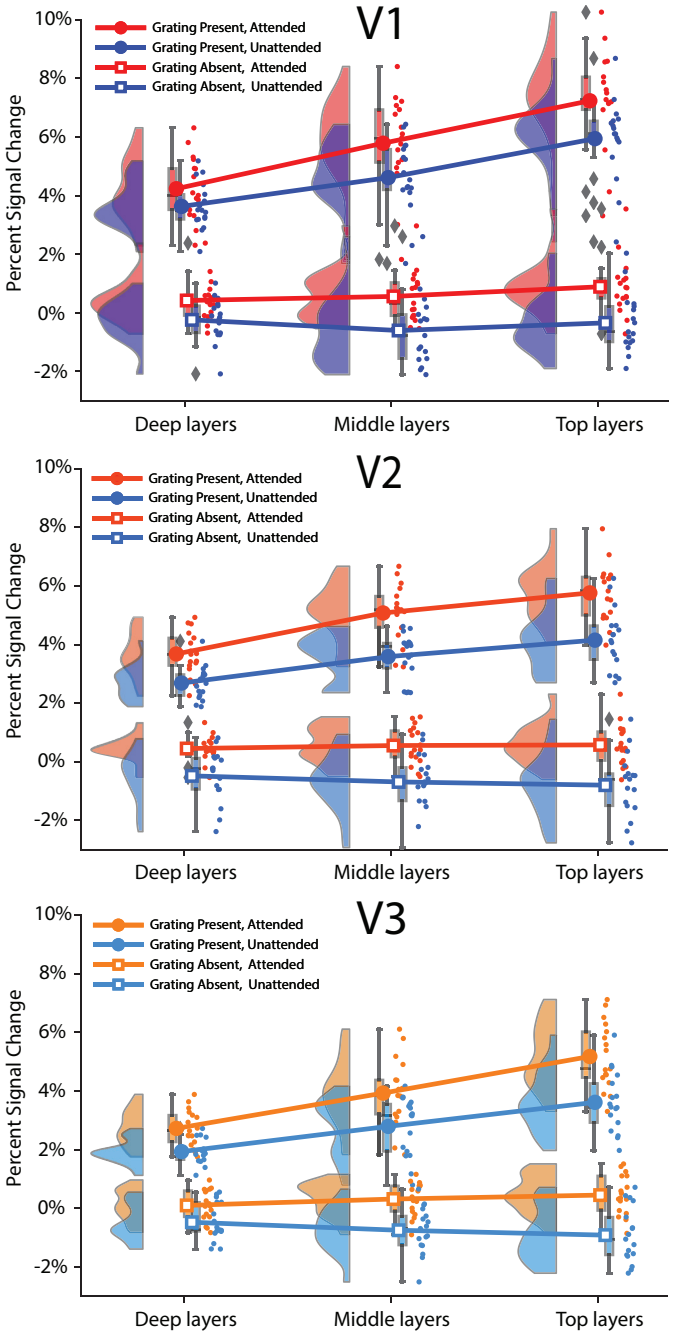

Figure 5–Figure supplement 1. A control analysis that is identical to the main analysis but repeated with a smaller region of interest. Only the 300 highest activated vertices were included in the analysis.

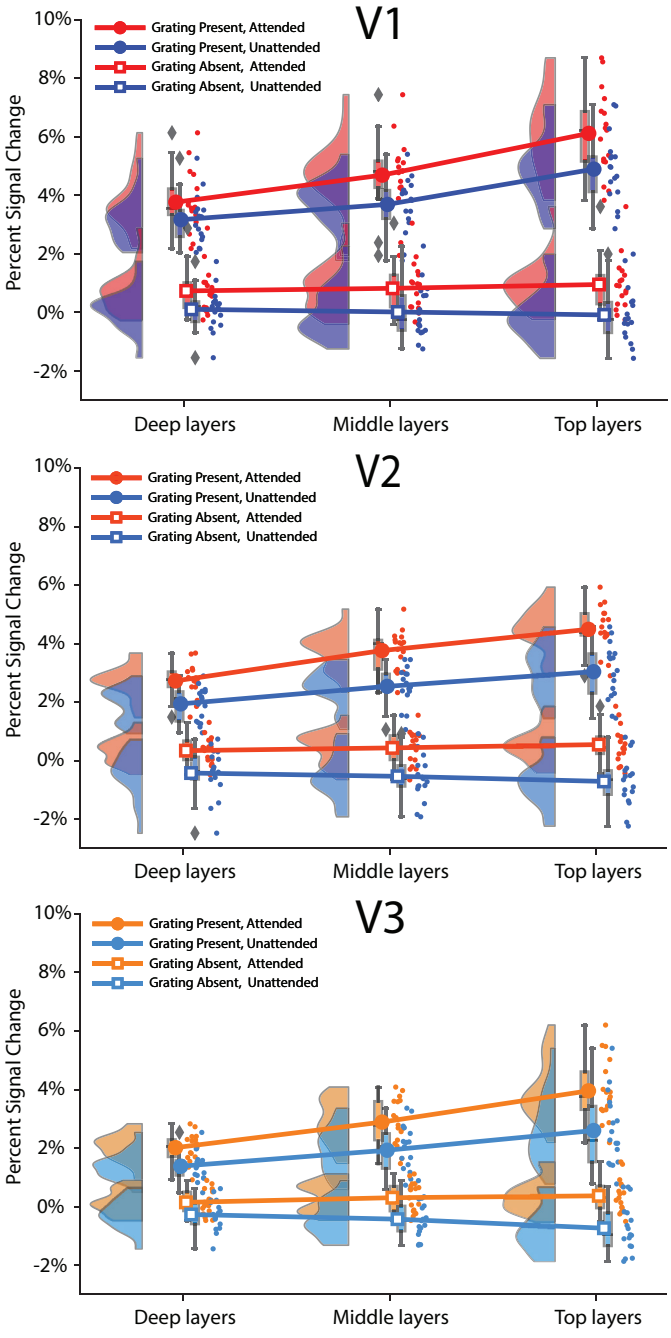

Figure 5–Figure supplement 2. A control analysis that is identical to the main analysis but repeated with a larger region of interest. Only the 900 highest activated vertices were included in the analysis.

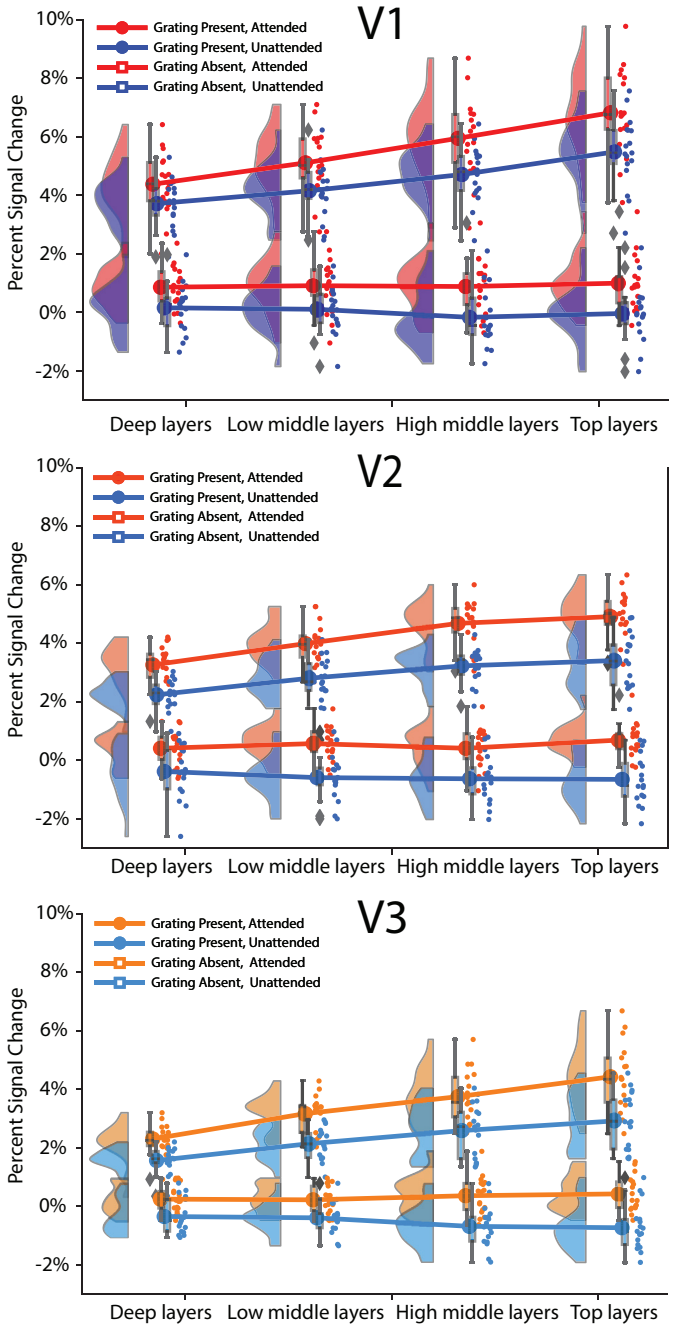

Figure 5–Figure supplement 3. A control analysis that is identical to the main analysis but repeated with four extracted layers instead of three.

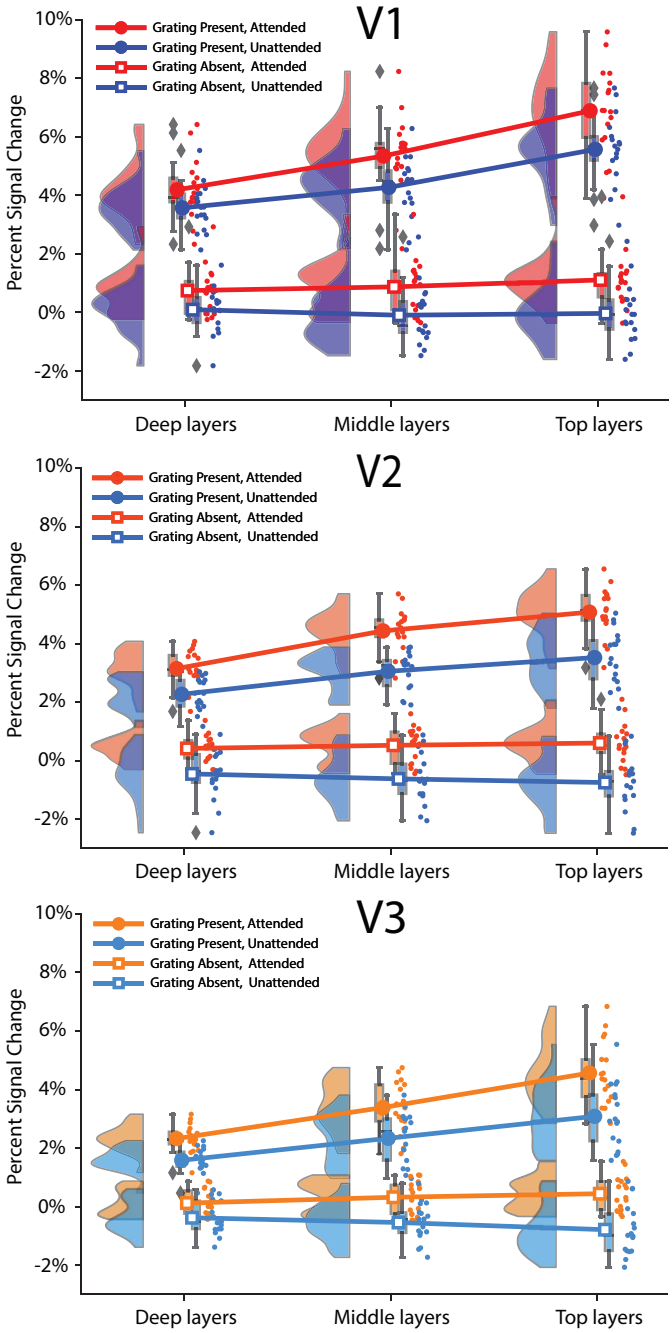

Figure 5–Figure supplement 4. A control analysis that is identical to the main analysis but repeated with an interpolation strategy to obtain laminar signal.

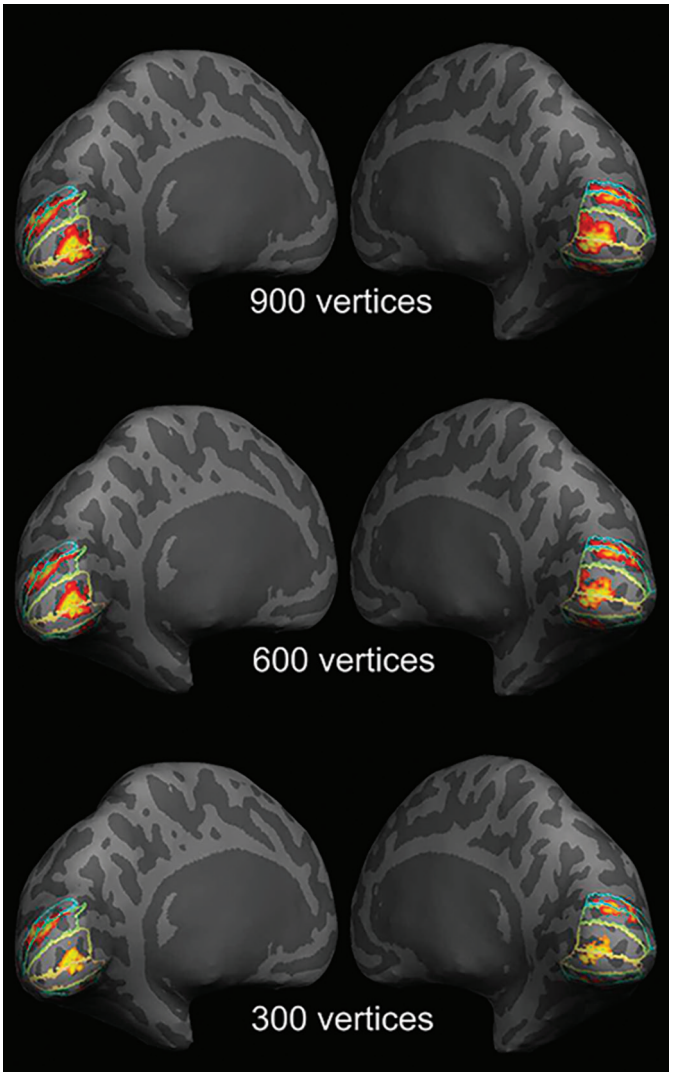

Figure 5–Figure supplement 5. Example of Regions of Interest on the inflated cortical surface for a representative subject. The label contours from top to bottom show dorsal V3, V2, and V1 and ventral V1, V2, and V3, in both hemispheres. The 600 most activated vertices (coloured area) per region were selected for the main analysis. The 300 and 900 vertices were used for control analyses in order to show that the effects are independent of size of region of interest.

